Title
Symmetric and antisymmetric resonances in a pair of metal-dielectric nanoshells: tunability and closed-form formulas

Journal
Journal of Nanophotonics, 4(1)

ISSN
1934-2608

Authors
Vallecchi, Andrea
Campione, Salvatore
Capolino, Filippo

Publication Date
2010-04-01

DOI
10.1117/1.3430112

Symmetric and antisymmetric resonances in a pair of metal-dielectric nanoshells: tunability and closed-form formulas

Andrea Vallecchi,[a,b] Salvatore Campione,[a] and Filippo Capolino[a]

[a] University of California, Irvine, Department of Electrical Engineering and Computer Science, Irvine, CA 92697

andrea.vallecchi@unisi.it, scampion@uci.edu, f.capolino@uci.edu

[b] University of Siena, Department of Information Engineering, 53100 Siena, Italy

Abstract. Resonances of symmetric and antisymmetric polarization states in tightly coupled nanoshell particles made of either a metallic core and a dielectric shell or, vice versa, a dielectric core and a metallic shell were analyzed at optical frequencies. The investigation was performed by using the single dipole approximation (SDA) with all the dynamical retarded field terms included. Furthermore, analytic formulas for the four possible resonances were derived for the first time by retaining only the static (non-retarded) term in the dipolar field expression. The image principle was used to distinguish a priori between symmetric and antisymmetric modes and for full-wave simulations performed to confirm the identification of resonances achieved by the SDA. It was observed that the resonance frequencies of a pair of nanoshells can be tuned over a wide range of wavelength/frequencies by varying the relative dimensions of the core and shell. This makes this kind of particle pairs suited very well to be adopted either as constituents of metamaterials or to enhance local fields when operating frequencies range from the visible to the infrared spectral regions.

Keywords: nanoshells, plasmonics, metamaterials, scattering.

1 INTRODUCTION

The physical mechanism underlying the enhancement of the electromagnetic field intensities around subwavelength-size metal particles and their increased absorption and scattering cross sections is the coupling between the photons of incident light at certain frequencies and resonant collective oscillations of free electrons at the metal surface, referred to as localized surface plasmon resonances [1,2]. Surface-enhanced Raman scattering (SERS) is an important example in which metallic nanoparticles could be employed because of the strong enhancement of the scattered field [3,4].

The plasmonic properties of a nanostructure depend dramatically on its size and shape. Plasmonic pairs of various nanoparticles have been studied experimentally and theoretically, with the general observation that for incident light polarized along the dimer (pair) axis, a red-shift of the longitudinal plasmon resonance occurs with decreasing nanoparticle separation [5,6]. Pairs of plasmonic nanoparticles constitute a simple system to achieve strong enhancements of near fields or scattering at optical frequencies, that could also be employed in SERS. Plasmon theory applied to nanoparticle pairs has led to the understanding of pair plasmon modes as symmetric and antisymmetric hybridized modes of the characteristic plasmons of the constituent nanoparticles [7]. The use of nanosphere pairs and rings has been also proposed to create artificial magnetism [8-14], similarly to what has been proposed based on pairs of rods [15-17]. A particularly useful nanoparticle is the metal-dielectric nanoshell [1,18]. A dielectric core-metal shell nanoparticle is a composite nanoparticle whose optical resonance can be designed in a controlled manner [18,19]. By varying the relative dimensions

Received 11 Jan 2010; accepted 7 Apr 2010; published 27 Apr 2010 [CCC: 19342608/2010/$25.00]

of the core and shell, the optical resonance of such a nanoparticle can be varied over hundreds of nanometers in wavelength, across the visible and into the infrared region of the spectrum. For example, the tunability of a nanoshell resonance is useful for SERS applications [20-22]. Moreover, using nanoshells with active materials could result in a reduction of the losses in pairs of plasmonic nanoparticles [23]. Whereas plasmonic properties of individual nanoshell particles are well understood, few studies have been performed on the optical properties of nanoshell pairs [20,24-27].

In this paper, we show how tuning of both symmetric and antisymmetric resonance frequencies in pairs of electromagnetically coupled nanoparticles can be achieved by exploiting the additional degree of freedom provided by using metal-dielectric nanoshells, in contrast to using single-metal nanoparticles. To this aim, the nanoparticles are modeled by using the single dipole approach (SDA) [1], which has been summarized in Ref. 28. We also provide closed-form formulas representing the four resonance frequencies in a pair of nanoshells by combining the SDA with a quasistatic approximation for the field emitted by the dipole, valid for small and very close nanoshells. Finally, the excitation of the resonant modes identified by the SDA by an illuminating wave field is discussed presenting some full-wave simulation results.

2 STATEMENT OF THE PROBLEM

Figure 1 shows the two considered nanoshell pair configurations, where r_1 and r_2 are the core and shell radii, respectively, and d is the center-to-center distance between the two particles. The nanoshells are made up of either a metal core and a dielectric shell (Fig. 1(a)) or a dielectric core and a metal shell (Fig. 1(b)).

The purpose of this paper is to characterize the resonant behavior of these two structures by varying the structure parameters described above, stressing resonances' tunability.

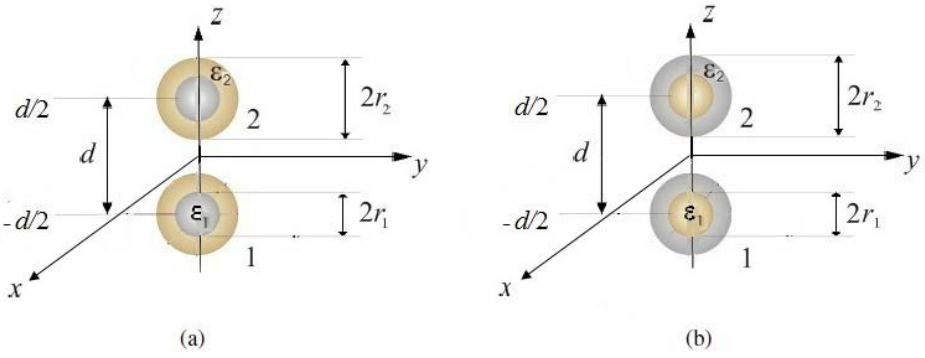

Fig. 1. Geometry of a pair of tightly coupled metallic nanoshells. (a) Metal core and dielectric shell. (b) Dielectric core and metal shell.

3 FORMULATION

In this section, we derive two scalar equations for predicting the resonance modes of a pair of nanoshells, resulting into simple closed-form expressions for the resonance frequencies associated to the structures. These expressions also permit to account for the presence of a host medium with permittivity different from that of free space.

3.1 Electromagnetic modes of two coupled metallic spheres

The electric field at the position $\boldsymbol{r}_2$ ($=\hat{\boldsymbol{z}}\,d/2$ in Fig. 1) generated by a dipole with dipole moment $\boldsymbol{p}_1$ placed at the position $\boldsymbol{r}_1$ ($=-\hat{\boldsymbol{z}}\,d/2$ in Fig. 1) can be expressed by means of the dyadic Green's function (electromagnetic fields are assumed to be time harmonic with an $e^{-i\omega t}$ time variation)

$$\boldsymbol{E}(\boldsymbol{r}_2)=\underline{\boldsymbol{G}}(\boldsymbol{r}_2,\boldsymbol{r}_1)\cdot\boldsymbol{p}_1\ , \tag{1}$$

where the expression of the dyadic Green's function is given in Refs. 28 and 29. Note that because of reciprocity $\underline{\boldsymbol{G}}(\boldsymbol{r}_2,\boldsymbol{r}_1)=\underline{\boldsymbol{G}}(\boldsymbol{r}_1,\boldsymbol{r}_2)$. When a subwavelength metallic nanoshell is immersed in an electric field, its induced dipole moment $\boldsymbol{p}$ is given by $\boldsymbol{p}=\varepsilon_0\varepsilon_h\alpha\boldsymbol{E}$, where $\boldsymbol{E}$ is the local electric field at the particle location. For nanosphere shells, the static expression for the inverse polarizability is given by [1,22,30]

$$\frac{1}{\alpha}=\frac{1}{4\pi r_2^3}\frac{(\varepsilon_2+2\varepsilon_h)(\varepsilon_1+2\varepsilon_2)+2\beta(\varepsilon_2-\varepsilon_h)(\varepsilon_1-\varepsilon_2)}{(\varepsilon_2-\varepsilon_h)(\varepsilon_1+2\varepsilon_2)+\beta(2\varepsilon_2+\varepsilon_h)(\varepsilon_1-\varepsilon_2)}-i\frac{k_h^3}{6\pi}\,, \tag{2}$$

where ε_h is the relative permittivity of the host medium, ε_1 is the relative permittivity of the core (of radius r_1), and ε_2 is the relative permittivity of the shell (of external radius r_2). Furthermore, $\beta=\rho^3$, with $\rho=r_1/r_2$ and $k_h=\omega\sqrt{\varepsilon_h}/c=k_0\sqrt{\varepsilon_h}$ is the host wavenumber, where k_0 denotes the free space wavenumber. The last imaginary term in (2) has been introduced to account for particle radiation [1,28]. The Drude model is used to describe the metal permittivity

$$\varepsilon_m=\varepsilon_\infty-\frac{\omega_p^2}{\omega(\omega+i\gamma)}\,, \tag{3}$$

where ω_p is the plasma angular frequency, γ the damping term, and ε_∞ is a "high frequency" permittivity determined to match experimental data. Here, for silver we use the values provided in Refs. 8 and 31: $\varepsilon_\infty=5$, $\omega_p=1.37\times10^{16}$ rad/s, and $\gamma=27.3\times10^{12}$ s^{-1}.

We aim at finding the eigenvalues and eigenvectors of the two-sphere system (Fig. 1) by solving the coupled equations

$$\boldsymbol{E}(\boldsymbol{r}_2)=\underline{\boldsymbol{G}}(\boldsymbol{r}_2,\boldsymbol{r}_1)\cdot\boldsymbol{p}_1,\quad \boldsymbol{E}(\boldsymbol{r}_1)=\underline{\boldsymbol{G}}(\boldsymbol{r}_1,\boldsymbol{r}_2)\cdot\boldsymbol{p}_2\,, \tag{4}$$

with the information that $\boldsymbol{p}_2=\varepsilon_0\varepsilon_h\alpha\boldsymbol{E}(\boldsymbol{r}_2)$ and $\boldsymbol{p}_1=\varepsilon_0\varepsilon_h\alpha\boldsymbol{E}(\boldsymbol{r}_1)$. Combining these equations with (4), and following the procedure outlined in Ref. 14, we obtain two scalar equations, one for the transverse polarization (electric dipole moment orthogonal to the axis of the pair, z) and one for the longitudinal polarization (electric dipole moment along the axis of the pair).

The resonances for the two transverse antisymmetric/symmetric polarizations are found by solving numerically

$$\left(c_1 \pm \frac{1}{\varepsilon_0 \varepsilon_h \alpha}\right) = 0, \qquad c_1 = \frac{e^{ik_h d}}{4\pi\varepsilon_h \varepsilon_0}\left(\frac{k_h^2}{d} + \frac{ik_h}{d^2} - \frac{1}{d^3}\right), \tag{5}$$

where the "+" sign is for the antisymmetric mode ($\boldsymbol{p}_2 = -\boldsymbol{p}_1$), whereas the "−" sign is for the symmetric one ($\boldsymbol{p}_2 = \boldsymbol{p}_1$). Analogously, the resonances for the longitudinal antisymmetric/symmetric polarizations are found from

$$\left(c_3 \pm \frac{1}{\varepsilon_0 \varepsilon_h \alpha}\right) = 0, \qquad c_3 = -\frac{e^{ik_h d}}{4\pi\varepsilon_h \varepsilon_0}\left(\frac{2ik_h}{d^2} - \frac{2}{d^3}\right). \tag{6}$$

The eigenvectors $\boldsymbol{p}_1$ and $\boldsymbol{p}_2$ associated to the four resonances are shown in Fig. 2. The two eigenfrequencies f_{t1} and f_{t2} associated to the two *transverse* (with respect to the pair axis) resonances in Figs. 2(b) and 2(c) are solutions of equation (5), with the "+" (antisymmetric) and "−" (symmetric) sign, respectively. The two eigenfrequencies $f_{\ell 1}$ and $f_{\ell 2}$ associated to the two *longitudinal* (parallel to the pair axis) resonances in Figs. 2(d) and 2(a) are solutions of equation (6), with the "+" (antisymmetric) and "−" (symmetric) sign, respectively.

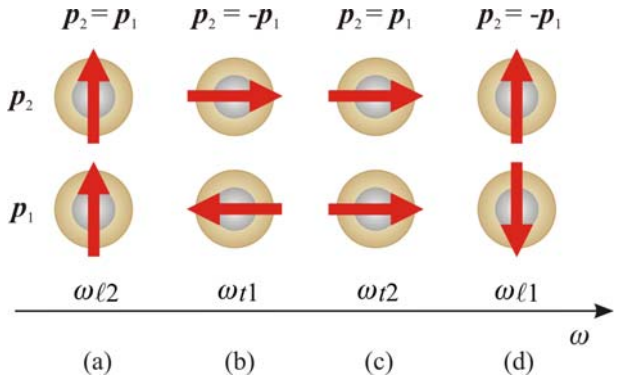

Fig. 2. Four possible resonance states in a pair of nanoshells. Both transverse (t) and longitudinal (ℓ) resonance modes exhibit symmetric and antisymmetric configurations. The resonance order is the limiting case valid under the quasistatic (QS) approximation.

3.2 Quasistatic (QS) field approximation for resonance modes of two metallic nanospheres

Here we are interested in deriving the analytical expressions for the resonances associated to a nanoshell pair. If the particles are small compared to the free space wavelength, it is possible to replace some electrodynamic terms by electrostatic ones. In SDA calculations, this is equivalent to setting $k_h = 0$ in (2), (5), and (6) (see also Ref. 28) but keeping the correct frequency-dependent dielectric constant ε_m in (3). This approximation applies specifically to the dynamics of a single particle, but it is here used in combination with the SDA method to describe the electromagnetic behaviour of a pair of nanoshells [32,33]. Therefore, after neglecting the dynamic terms (in other words we keep only the $1/d^3$ terms in (5) and (6)) and

by taking into account that $\gamma << \omega_p$, (5) and (6) are solved analytically for the resonant angular frequencies leading to the expressions for transverse and longitudinal polarizations for the two cases of metal core-dielectric shell and dielectric core-metal shell.

3.2.1 Metal core – dielectric shell

For the *transverse* polarization, the procedure described above leads to

$$\omega_{t1,2} = \frac{\omega_p}{\sqrt{\varepsilon_\infty + \varepsilon_2 \dfrac{b' - b''(\pm\delta)}{a' - a''(\pm\delta)}}} - i\frac{\gamma}{2}, \tag{7}$$

where $\delta = (r_2/d)^3$, and the upper/lower sign applies to the antisymmetric/symmetric transverse polarization. The formula coefficients are

$$a' = 2\beta(\varepsilon_2 - \varepsilon_h) + (\varepsilon_2 + 2\varepsilon_h), \quad a'' = \beta(2\varepsilon_2 + \varepsilon_h) + (\varepsilon_2 - \varepsilon_h), \tag{8}$$

and

$$b' = -2\beta(\varepsilon_2 - \varepsilon_h) + 2(\varepsilon_2 + 2\varepsilon_h), \quad b'' = -\beta(2\varepsilon_2 + \varepsilon_h) + 2(\varepsilon_2 - \varepsilon_h). \tag{9}$$

For the *longitudinal* polarization instead, the closed-form expression for the antisymmetric (upper sign) and symmetric (lower sign) resonances is:

$$\omega_{\ell 1,2} = \frac{\omega_p}{\sqrt{\varepsilon_\infty + \varepsilon_2 \dfrac{b' - b''(\mp 2\delta)}{a' - a''(\mp 2\delta)}}} - i\frac{\gamma}{2}. \tag{10}$$

Note that expression (10) is the same as (7) after replacing δ by -2δ. For $\varepsilon_h = 1$ (nanoshells in vacuum), and $\varepsilon_1 = \varepsilon_2$ (core and shell made of the same material) these expressions coincide with those in Refs. 14 and 34.

3.2.2 Dielectric core – metal shell

The procedure previously described leads to the following closed-form expression for the transverse antisymmetric (upper sign) and symmetric (lower sign) modes

$$\omega_{t1,2} = \frac{\omega_p}{\sqrt{2}} \sqrt{\frac{a'(\pm\delta) + a'' - \sqrt{\left[b'(\pm\delta) + c''\right]^2 - 36\varepsilon_1\varepsilon_h\beta(\delta^2 \pm \delta - 2)}}{(d' + b''\varepsilon_\infty)(\pm\delta) - d'' + c'\varepsilon_\infty}} - i\frac{\gamma}{2}, \tag{11}$$

whereas, for the longitudinal antisymmetric (upper sign) and symmetric (lower sign) modes, we have

$$\omega_{\ell 1,2} = \frac{\omega_p}{\sqrt{2}} \sqrt{\frac{a'(\mp 2\delta) + a'' - \sqrt{\left[b'(\mp 2\delta) + c''\right]^2 - 36\varepsilon_1\varepsilon_h\beta(4\delta^2 \mp 2\delta - 2)}}{(d' + b''\varepsilon_\infty)(\mp 2\delta) - d'' + c'\varepsilon_\infty}} - i\frac{\gamma}{2}, \tag{12}$$

with

$$a' = \varepsilon_h(\beta+2) - \varepsilon_1(2\beta+1) + 4\varepsilon_\infty(\beta-1), \quad a'' = 2\varepsilon_h(\beta+2) + \varepsilon_1(2\beta+1) - 4\varepsilon_\infty(\beta-1), \tag{13}$$

$$b^{',''} = \varepsilon_h(\beta+2) \pm \varepsilon_1(2\beta+1), \quad c^{',''} = 2\varepsilon_h(\beta+2) \pm \varepsilon_1(2\beta+1), \tag{14}$$

$$d' = (\beta-1)(2\varepsilon_\infty^2 - \varepsilon_1\varepsilon_h), \quad d'' = 2(\beta-1)(\varepsilon_\infty^2 + \varepsilon_1\varepsilon_h). \tag{15}$$

As in the previous case, note that (12) is the same as (11) after replacing δ by -2δ.

4 RESULTS

We show the resonant frequencies for the dynamic, fully retarded case ("Dyn", continuous lines in Figs. 3-8) in comparison with those obtained by the quasistatic approximation ("QS", dashed lines) for variable geometrical parameters. Distribution of electromagnetic fields at resonances are then illustrated by means of full-wave simulations. All presented numerical results refer to a pair of nanoshells lying in free space (i.e., $\varepsilon_h = 1$).

4.1 Analysis of resonant frequencies

The real and imaginary parts of the four resonance frequencies of a pair of nanoshells are plotted versus the ratio of the core and shell radii $\rho = r_1/r_2$ in Fig. 3 for the metallic core-dielectric shell case, and in Fig. 4 for the dielectric core-metallic shell one, keeping the nanoshells center-to-center distance at $d = 125$ nm and the shell radius at $r_2 = 50$ nm. Figures 5 and 6 plot the same resonance frequencies versus the ratio $\tau = r_2/d$ of the nanoshell radius to the center-to-center distance, with fixed $d = 75$ nm and $\rho = r_1/r_2 = 0.8$ (i.e., the nanoshell radius r_2 is variable here). Figures 7 and 8 plot the same quantities versus the ratio $\tau = r_2/d$, at fixed shell radius $r_2 = 40$ nm and $\rho = r_1/r_2 = 0.8$ (i.e., the center-to-center distance between the nanoshells is variable here).

The imaginary part of the frequency solutions represents the total amount of material and radiation losses. Note that f_{t2} and $f_{\ell 2}$, the resonances of the symmetric modes in Figs. 2(c) and 2(a), have a larger imaginary part than f_{t1} and $f_{\ell 1}$, the resonances of the antisymmetric modes in Figs. 2(b) and 2(d). This is because radiation losses for symmetric modes are significantly larger since the pair of nanoshells radiates like a dipole, whereas the two radiation contributions associated to the two antisymmetric (opposite) dipoles tend to cancel out. In other words, the transverse resonance for the antisymmetric pair tends to radiate like a magnetic dipole [11,14] plus an electric quadrupole [11]. Indeed, the antisymmetric mode is associated to a current loop (magnetic dipole) and it is a classic result of antenna theory that a small loop radiates less than a small dipole of same current and dimension. Note that the *transverse* antisymmetric resonance frequency f_{t1} is smaller than the symmetric one f_{t2}, for all cases considered. Also, note that the *longitudinal* symmetric resonance frequency $f_{\ell 2}$ is smaller than the antisymmetric one $f_{\ell 1}$, except for very small values of $\tau = r_2/d$. And in general (but not always), the resonances are ordered as $f_{\ell 2} < f_{t1} < f_{t2} < f_{\ell 1}$. It is also noted that at small ratios $\tau = r_2/d$ the real parts of the four resonance frequencies tend to be similar, and close to the resonance of a single particle, due to weaker coupling.

The results obtained by including in the calculations all the dynamic field components of the dipole radiation (5) and (6), which are denoted as "Dyn", are compared with those

computed by the closed-form expressions (7) and (10)−(12) derived by retaining only the quasistatic (denoted as QS) dipolar field terms as described in Sec. 3.2.

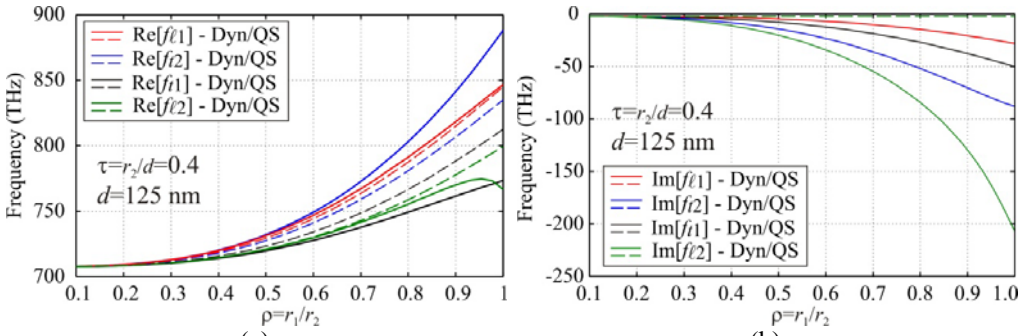

(a) (b)

Fig. 3. Real and imaginary parts of the four resonance frequencies versus ratio of radii, for a sphere distance d = 125 nm (r_2 = 50 nm) for the metallic core-dielectric shell structure. "Dyn" means that all dipolar dynamic field components are considered; "QS" means that only the static component $1/d^3$ of the dipolar field is considered.

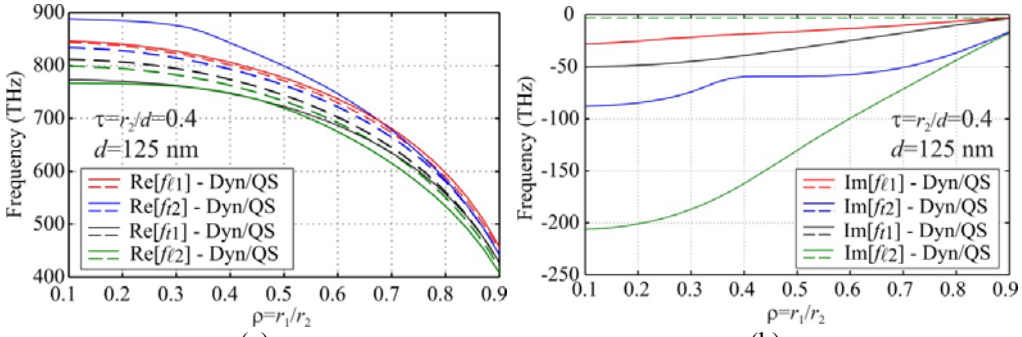

(a) (b)

Fig. 4. Real and imaginary parts of the four resonance frequencies versus ratio of radii, for a sphere distance d = 125 nm (r_2 = 50 nm) for the dielectric core-metallic shell structure.

From Fig. 3 one can notice that the dynamic and quasistatic solutions agree well for small values of the ratio of radii (with fixed $d = 125$ nm) for the case in Fig. 1(a), and for high values of the ratio of radii (with fixed $d = 125$ nm) for the case in Fig. 1(b). In general, the QS approximation is less accurate than the fully dynamic solution because it neglects the effect of retardation in the coupling mechanism between the two nanoshells and the $1/d$ and $1/d^2$ field terms. Therefore, the stronger the coupling between the two nanoshells is, the less accurate the QS results are. To illustrate this, in Figs. 5 and 6 we show that for larger shell radius r_2 (and therefore for larger scattered field) the QS approximation tends to diverge from the dynamic solution because it cannot correctly describe the interaction between the particles. On the other hand, in Figs. 7 and 8 (that show the resonant frequencies for varying $\tau = r_2/d$, at a fixed ratio of the core and shell radii $\rho = r_1/r_2 = 0.8$), the "QS" and "Dyn" solutions, though in general agreement with each other, show a small difference which is more or less independent from the distance d. This is because though the QS approximation for small d is expected to be better than for large d, the amount of coupling between the

nanoshells is inversely proportional to d, and the influence of the coupling on the estimation of the resonant frequencies affects the overall approximation.

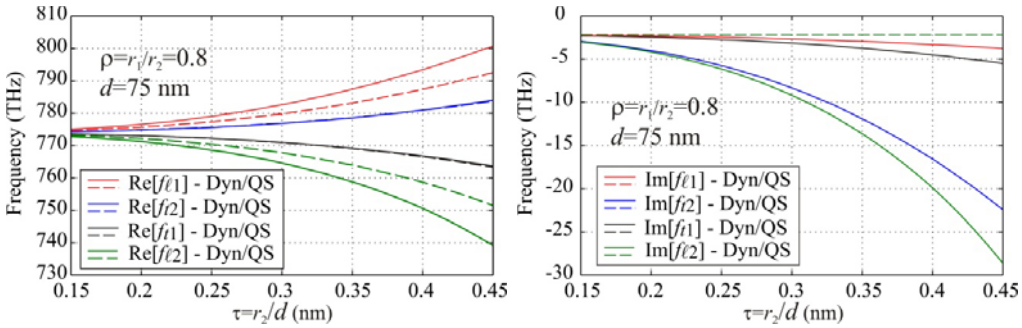

Fig. 5. Real and imaginary parts of the four resonance frequencies versus the ratio $\tau = r_2/d$ for fixed distance d = 75 nm between the nanoshells (i.e., the shell radius r_2 is variable) and $\rho = r_1/r_2 = 0.8$ for the metallic core-dielectric shell structure.

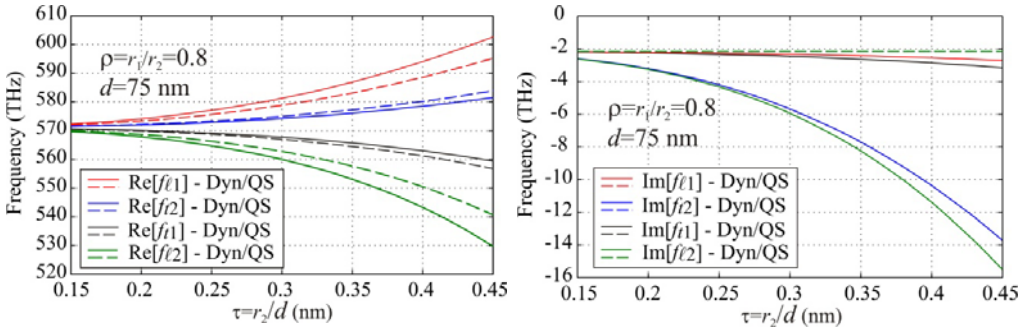

Fig. 6. Real and imaginary parts of the four resonance frequencies versus the ratio $\tau = r_2/d$ for fixed distance d = 75 nm between the nanoshells (i.e., the shell radius r_2 is variable) and $\rho = r_1/r_2 = 0.8$ for the dielectric core-metallic shell structure.

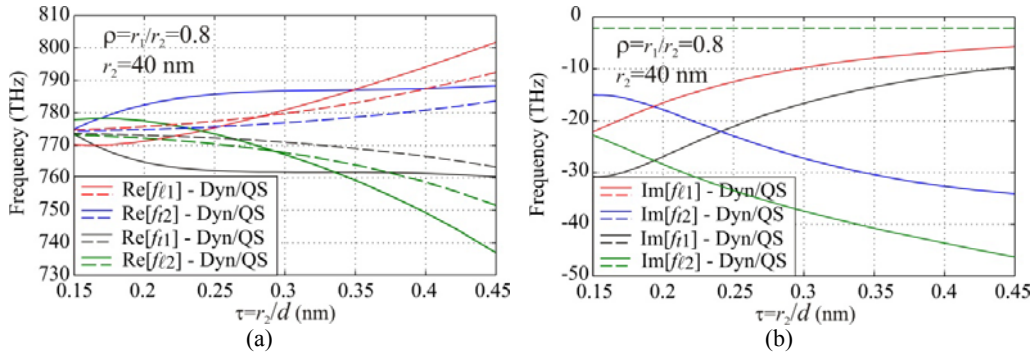

Fig. 7. Real and imaginary parts of the four resonance frequencies versus the ratio $\tau = r_2/d$ for fixed shell radius r_2 = 40 nm (i.e., the distance d between the nanoshells is variable) and $\rho = r_1/r_2 = 0.8$ for the metallic core-dielectric shell structure.

It can also be noted that in all cases the solutions employing only the quasistatic dipole terms provide a very poor prediction of the imaginary part of the resonant frequencies since the dipole radiation terms $1/d$ are not accounted for in the QS estimate. The QS prediction is indeed poorer for the symmetric resonances, where radiation is stronger. We recall that, as shown in Refs. 28 and 31, the SDA starts to fail when the center-to-center distance d of the two nanoshells is smaller than $3r_2$.

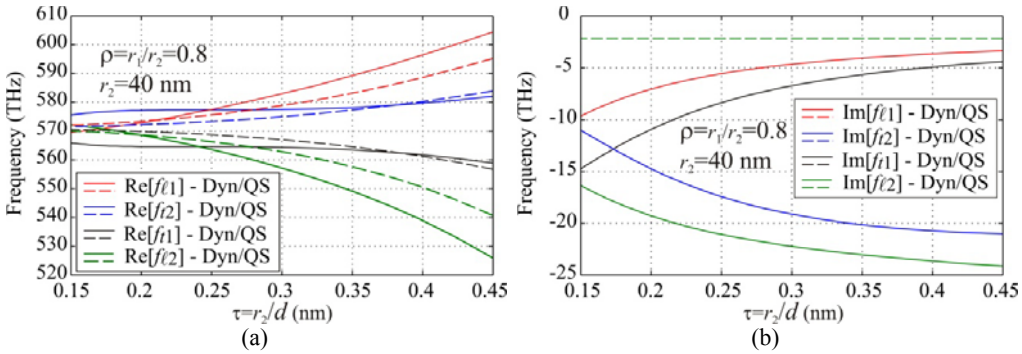

Fig. 8. Real and imaginary parts of the four resonance frequencies versus the ratio $\tau = r_2/d$ for fixed shell radius r_2 = 40 nm (i.e., the nanoshell distance d is variable) and $\rho = r_1/r_2 = 0.8$ for the dielectric core-metallic shell structure.

4.2 Full-wave results

The above concepts are here tested by comparing results obtained by the SDA with those by the full-wave solver CST Microwave Studio. Also in this case we observe the excitation of the antisymmetric and symmetric modes. These are excited by using either a pair of antisymmetric or symmetric (with respect to the electric field) plane waves, arriving from the $+z$ and $-z$ directions, or a single plane wave coming from $+z$. The incoming electric field is polarized along y for all considered excitations. Figure 9(a) shows the magnitude of the y-component of the electric field at the center of the nanoshells at $\boldsymbol{r}_1 = -\hat{\boldsymbol{z}}d/2$ and $\boldsymbol{r}_2 = \hat{\boldsymbol{z}}d/2$, excited by the plane wave pair, for the dielectric core-metallic shell structure. When using the SDA, the field $\boldsymbol{E}_i$ at a center of a nanoshell i=1,2 is found by using the expression

$$\boldsymbol{p}_i = \frac{4}{9}\pi r_2^3 \frac{\varepsilon_0}{\varepsilon_2}\left[(\varepsilon_2 - \varepsilon_h)(\varepsilon_1 + 2\varepsilon_2) + \beta(2\varepsilon_2 + \varepsilon_h)(\varepsilon_1 - \varepsilon_2)\right]\boldsymbol{E}_i\,, \tag{16}$$

once the nanoshell equivalent dipole polarization $\boldsymbol{p}_i$ has been determined by using the SDA method outlined in Ref. 14. The antisymmetric excitation has a null of the electric field at z = 0 and excites only the antisymmetric mode that has a magnitude peak, which corresponds to the transverse antisymmetric resonance f_{t1}, at f = 565 THz when using the SDA and at f = 547 THz when using CST. The blue shift of the SDA compared to the CST full wave results is in agreement with previous observations [28]. The symmetric excitation has a maximum of the electric field at z = 0 and excites only the symmetric mode that has a peak, denoting the transverse symmetric resonance f_{t2}, at f = 577 THz when using the SDA and at f = 565 THz when using CST. These peak location frequency values (obtained with the SDA and CST) have to be compared with the resonance frequencies obtained by solving equation (5), based on the static polarizability expression (2), that yields $f_{t1} = 564.8$ THz and $f_{t2} = 576.8$ THz; they have to be compared as well with the values obtained when using the formula (11),

based on the static dipole expressions and the static polarizability expression (2), which yields $f_{t1} = 564.5$ THz and $f_{t2} = 577.2$ THz. From these comparisons we can conclude that though the SDA, with the static or quasi-static polarizability, fails to predict the exact resonant frequencies, it still provides useful insight in the coupling mechanism of nanoshell pairs. Indeed, by using a more accurate expression for the polarizability based on the Lorenz-Mie theory [1], we expect that the accuracy of SDA could be greatly improved [28,35].

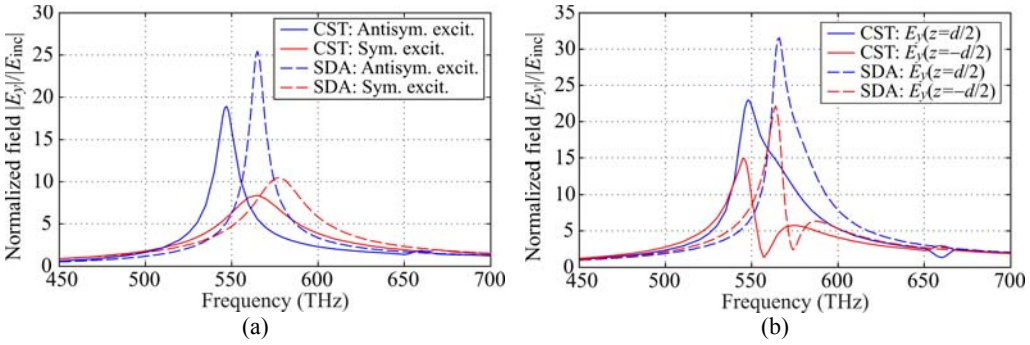

Fig. 9. Magnitude of the *y*-component of the electric field at the center of the shells, excited by (a) a pair of antisymmetric or symmetric plane waves arriving from the +*z* and –*z* directions, and (b) by a single plane wave coming from +*z*, for the dielectric core-metallic shell structure. Shell radius r_2=35 nm, ratio of the radii $\rho = r_1/r_2 = 0.8$ and center-to-center distance d =100 nm.

The electric field at the center of each nanoshell induced by a *single* normally incident plane wave polarized along *y*, is shown in Fig. 9(b), by using the SDA and CST. The field $\boldsymbol{E}_2$ at the center of the upper nanoshell exhibits two peaks, associated to the antisymmetric and symmetric modes, whereas the field $\boldsymbol{E}_1$ at the center lower nanoshell exhibits only the strongest peak associated to the antisymmetric mode. In fact, the superposition of the antisymmetric and symmetric resonant modes with similar amplitudes, because their peaks are located at close frequencies for the considered configuration, and opposite phases, make the field at the lower nanoshell almost completely vanishes in the vicinity of the higher frequency (symmetric) resonance. The electric and magnetic field distributions induced in a pair of nanoshells by a *single* normally incident plane wave polarized along *y* at frequencies *f* = 547 THz and *f* = 565 THz, close to the transverse antisymmetric and symmetric resonances, respectively, are illustrated in Fig. 10, where the arrow plots representing the magnitude of the electric field vector are superimposed to the color maps of the magnetic field intensity. The shell radius is r_2=35 nm, the ratio of the radii $\rho = r_1/r_2 = 0.8$ and the center-to-center distance is d =100 nm. The direction of the electric field is consistent with the orientation of the dipole eigenvectors for the transverse resonance modes deduced by the SDA in Sec. 3.1. Consistently with Fig. 9(b), close to the transverse antisymmetric resonance (Fig. 10(a)) the magnitude of the electric field at the lower nanoshell appears to be comparable with that at the upper nanoshell, whereas at the symmetric resonance frequency (Fig. 10(b)) it is considerably smaller.

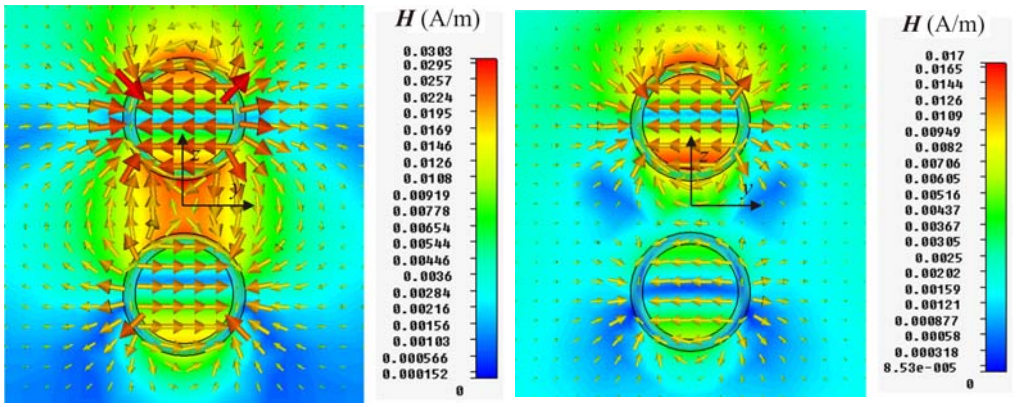

(a) (b)

Fig. 10. Electric (y-z plane) and magnetic (along *x*) field distributions for a pair of silver nanoshells, with shell outer radius r_2=35 nm, ratio of the radii $\rho = r_1/r_2 = 0.8$ and center-to-center distance d =100 nm, for the dielectric core-metallic shell structure. (a) Antisymmetric resonance mode excited by a single plane wave coming from +z at f = 547 THz (note the strong magnetic field between the two spheres); (b) symmetric resonance mode excited by a single plane wave at f = 565 THz.

5 CONCLUSION

In this paper we have shown how pairs of tightly coupled nanoshells offer the possibility of wide control of resonance frequencies and so their tunability, achievable by varying geometrical parameters. We have derived closed-form formulas for predicting resonance frequencies, based on a quasi-static approximation, and we have compared these results to the solution comprehensive of all retarded field terms in the single dipole approximation.

Moreover, these structures are shown to be able to support an antisymmetric mode that can be interpreted as an effective magnetic dipole; therefore, they could be used for providing artificial magnetism in metamaterials that may support backward propagation or have equivalent high/low characteristic wave impedance.

Acknowledgments

We thank Computer Simulation Technology (CST) for providing us their simulation tool that was instrumental in this analysis.

References

[1] C. F. Bohren and D. R. Huffman, *Absorption and Scattering of Light by Small Particles*, Wiley, New York (1983).

[2] S. A. Maier and H. A. Atwater, "Plasmonics: Localization and guiding of electromagnetic energy in metal/dielectric structures," *J. Appl. Phys.* **98**, 011101 (2005) [doi:10.1063/1.1951057].

[3] A. Wokaun, J. P. Gordon, and P. F. Liao, "Radiation damping in surface-enhanced Raman scattering," *Phys. Rev. Lett.* **48**, 957-960 (1982) [doi:10.1103/PhysRevLett.48.957].

[4] H. Kneipp, K. Kneipp, and M. Moskovits, *Surface-enhanced Raman Scattering: Physics and Applications*, Springer, Berlin (2006) [doi:10.1007/3-540-33567-6].

[5] W. Rechberger, A. Hohenau, A. Leitner, J. R. Krenn, B. Lamprecht, and F. R. Aussenegg, "Optical properties of two interacting gold nanoparticles," *Opt. Commun.* **220**, 137–141, May (2003) [doi:10.1016/S0030-4018(03)01357-9].

[6] L. Gunnarsson, T. Rindzevicius, J. Prikulis, B. Kasemo, M. Kall, S. Zou, and G. Schatz, "Confined plasmons in nanofabricated single silver particle pairs: Experimental observations of strong interparticle interactions," *J. Phys. Chem. B* **109**, 1079–1087 (2005) **[**doi:10.1021/jp049084e**]**.

[7] P. Nordlander, C. Oubre, E. Prodan, K. Li, and M. I. Stockman, "Plasmon hybridization in nanoparticle dimers," *Nano Lett.* **4**, 899-903 (2004) [doi:10.1021/nl049681c].

[8] A. Alù, A. Salandrino, and N. Engheta, "Negative effective permeability and left-handed materials at optical frequencies," *Opt. Expr.* **14**, 1557-1567 (2006) [doi:10.1364/OE.14.001557].

[9] A. Alù and N. Engheta, "Negative refraction in infrared and visible domains," Chapter 23 in *Theory and Phenomena of Metamaterials*, F. Capolino, Ed., pp. 23.1-23.28, CRC Press, Boca Raton, FL (2009).

[10] E. V. Ponizovskaya and A. M. Bratkovsky, "Ensembles of plasmonic nanospheres at optical frequencies and a problem of negative index behavior," *Appl. Phys. A* **87**, 175–179 (2007) [doi:10.1007/s00339-006-3861-0].

[11] A. Alù and N. Engheta, "Dynamical theory of artificial optical magnetism produced by rings of plasmonic nanoparticles," *Phys. Rev. B* **78**, 085112 (2008) [doi: 10.1103/PhysRevB.78.085112].

[12] A. Vallecchi, S. Steshenko, and F. Capolino, "Artificial magnetism at optical frequencies in composite materials made of particles with pairs of tightly coupled metallic nanospheres," in *Proc. URSI General Assembly*, Chicago, Illinois, USA, 7-16 Aug (2008).

[13] S. Steshenko, A. Vallecchi, and F. Capolino, "Electric and magnetic resonances in arrays with elements made of tightly coupled silver nanospheres," in *Proc. of Metamaterials'*, Pamplona, Spain, 21-26 Sep (2008).

[14] A. Vallecchi and F. Capolino, "Metamaterials based on pairs of tightly-coupled scatterers," Chapter 19 in *Theory and Phenomena of Metamaterials*, F. Capolino, Ed., pp. 19.1-19.47, CRC Press, Boca Raton, FL (2009)..

[15] V. A. Podolskiy, A. K. Sarychev, and V. M. Shalaev, "Plasmon modes in metal nanowires and left-handed materials," *J. Nonlinear Opt. Phys. Mater.* **11**, 65-74 (2002) [doi:10.1142/S0218863502000833].

[16] G. Dolling, C. Enkrich, M. Wegener, J. F. Zhou, C. M. Soukoulis, and S. Linden, "Cut-wire pairs and plate pairs as magnetic atoms for optical metamaterials," *Opt. Lett.* **30**, 3198-3200 (2005) [doi:10.1364/OL.30.003198].

[17] V. M. Shalaev, W. Cai, U. K. Chettiar, H. Yuan, A. K. Sarychev, V. P. Drachev, and A. V. Kildishev, "Negative index of refraction in optical metamaterials," *Opt. Lett.* **30**, 3356-3358 (2005) [doi:10.1364/OL.30.003356].

[18] P. Mulvaney, "Surface plasmon spectroscopy of nanosized metal particles," *Langmuir* **12**, 788-800 (1996) [doi:10.1021/la9502711].

[19] E. Prodan and P. Nordlander, "Structural tunability of the plasmon resonances in metallic nanoshells," *Nano Lett.* **3**, 543-547 (2003) [doi:10.1021/nl034030m].

[20] C. E. Talley, J. B. Jackson, C. Oubre, N. K. Grady, C. W. Hollars, S. M. Lane, T. R. Huser, P. Nordlander, and N. J. Halas, "Surface-enhanced Raman scattering from individual Au nanoparticles and nanoparticle dimer substrates," *Nano Lett.* **5**, 1569-1574 (2005) [doi:10.1021/nl050928v].

[21] M. Roca and A. J. Haes, "Silica-void-gold nanoparticles: temporally stable surface-enhanced Raman scattering substrates," *J. Am. Chem. Soc.* **130**, 14272-14279 (2008) [doi:10.1021/ja8059039].

[22] K. Tanabe, "Field enhancement around metal nanoparticles and nanoshells: A systematic investigation," *J. Phys. Chem. C* **112**, 15721-15728 (2008) [doi:10.1021/jp8060009].

[23] J. A. Gordon and R. W. Ziolkowski, "CNP optical metamaterials," *Opt. Expr.* **16**, 6692-6716 (2008) [doi:10.1364/OE.16.006692].
[24] D. W. Brandl, C. Oubre, and P. J. Nordlander, "Plasmon hybridization in nanoshell dimers," *J. Chem. Phys.* **123**, 024701 (2005) [doi:10.1063/1.1949169].
[25] P. K. Jain and M.A. El-Sayed, "Universal scaling of plasmon coupling in metal nanostructures: Extension from particle pairs to nanoshells," *Nano Lett.* **7**, 2854-2858 (2007) [doi:10.1021/nl071496m].
[26] J. B. Lassiter, J. Aizpurua, L. I. Hernandez, D. W. Brandl, I. Romero, S. Lal, J. H. Hafner, P. Nordlander, and N. J. Halas, "Close encounters between two nanoshells," *Nano Lett.* **8**, 1212-1218 (2008) [doi:10.1021/nl080271o].
[27] A. Vallecchi and F. Capolino, "Tunability of symmetric and antisymmetric resonances in metal-dielectric nanoshell pairs," in *Proc. of Metamaterials'*, London, UK, 30 Aug.- 4 Sep (2009).
[28] S. Steshenko and F. Capolino, "Single dipole approximation for modeling collections of nanoscatterers," Chapter 8 in *Theory and Phenomena of Metamaterials*, F. Capolino, Ed., pp. 8.1-8.17, CRC Press, Boca Raton, FL (2009).
[29] J. D. Jackson, *Classical Electrodynamics*, 3rd ed., Wiley, New York (1998).
[30] A. Sihvola, *Electromagnetic Mixing Formulas and Applications*, IEEE Publishing, London (1999).
[31] I. El-Kady, M. M. Sigalas, R. Biswas, K. M. Ho, and C. M. Soukoulis, "Metallic photonic crystals at optical wavelengths," *Phys. Rev. B* **62**, 15299-15302 (2000) [doi:10.1103/PhysRevB.62.15299].
[32] T. Jensen, L. Kelly, A. Lazarides, and G. Schatz, "Electrodynamics of noble metal nanoparticles and nanoparticle clusters," *J. Cluster Sci*. **10**, 295–317 (1999) [doi:10.1023/A:1021977613319].
[33] S. Y. Park and D. Stroud, "Surface-plasmon dispersion relations in chains of metallic nanoparticles: An exact quasistatic calculation," *Phys. Rev. B* **69**, 125418 (2004) [doi:10.1103/PhysRevB.69.125418].
[34] V. Myroshnychenko, J. Rodríguez-Fernández, I. Pastoriza-Santos, A. M. Funston, C. Novo, P. Mulvaney, L. M. Liz-Marzán, and F. J. García de Abajo, "Modelling the optical response of gold nanoparticles," *Chem. Soc. Rev.* **37,** 1792-1805 (2008) [doi:10.1039/b711486a].
[35] W. T. Doyle, "Optical properties of a suspension of metal spheres," *Phys. Rev. B* **39**, 9852–9858 (1989) [doi:10.1103/PhysRevB.39.9852].

Andrea Vallecchi: biography not available.

Salvatore Campione received his Laurea triennale degree (*cum laude*) in electrical engineering from Polytechnic of Turin, Italy in 2007 and his M.Sc. in electrical engineering from both Polytechnic of Turin, Italy and University of Illinois at Chicago, USA in 2009. He is currently a PhD student at University of California, Irvine, USA. His research interests include optical metamaterials, plasmonics in nanostructures and optical devices with super resolution.

Filippo Capolino received the Laurea degree (*cum laude*) and the Ph.D. degree in electrical engineering from the University of Florence, Italy, in 1993 and 1997, respectively. He is an Assistant Professor at the Department of Electrical Engineering and Computer Science of the University of California, Irvine, from July 2008. Previously he was an Assistant Professor at the Department of Information Engineering of the University of Siena, Italy. His research interests include metamaterials, micro and nanotechnology, antennas, and theoretical and applied electromagnetics in general. He is the Editor of the *Metamaterials Handbook*, CRC-Press, Boca Raton, FL, 2009.